Torsional Motion Due to Small-scale Geological Irregularities

M. Reza Ghayamghamian, IIEES

G. Reza Nouri, Mohaghegh Ardabili Univesity

IIEES

International Institute of Earthquake Engineering and Seismology

2nd IWGoRS, Czech Republic, Prague

Outlines

- Torsional motion from array measurements.
- Translation and torsion motion couplings.
- Observed torsion in Sendai.
- Sendai Seismic array.
- Estimation of Torsional motion using Sendai array data.
- Torsional motion variations around Sendai Basin.
- Numerical model for small-scale basin.
- Centrifuge testing for modeling small-scale basin.
- Conclusions

Torsional motion from array measurements

$$\ddot{\theta}(t) = \frac{1}{2}\left(\frac{\partial \ddot{u}(x,y,t)}{\partial y} - \frac{\partial \ddot{v}(x,y,t)}{\partial x}\right)$$

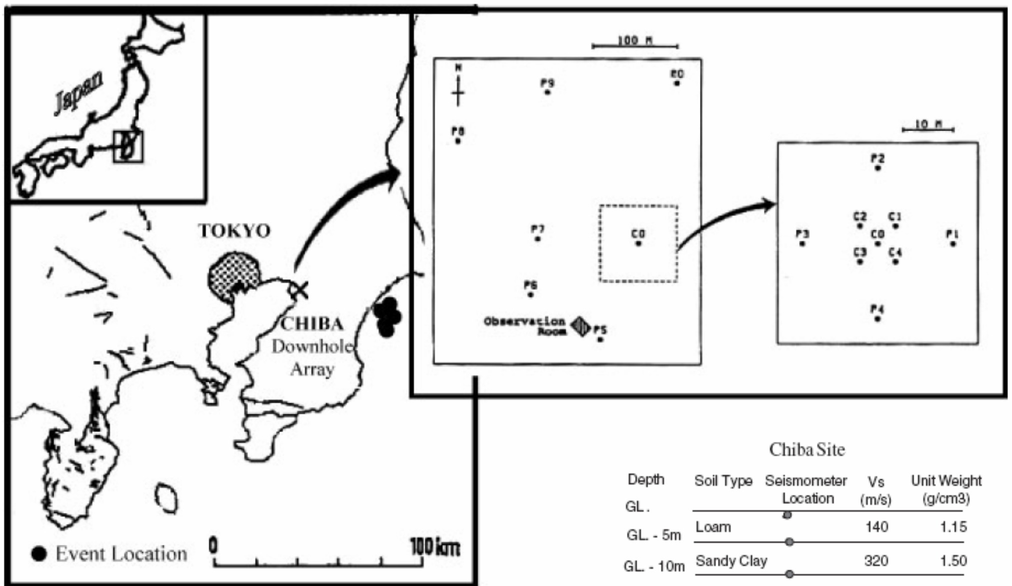

Figure 1. Map of Japan with location o

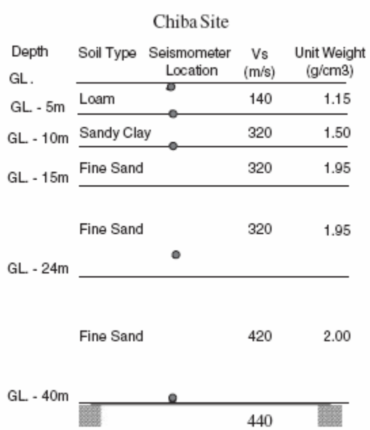

Figure 2. Soil profile at borehole C0 and position of seismometers

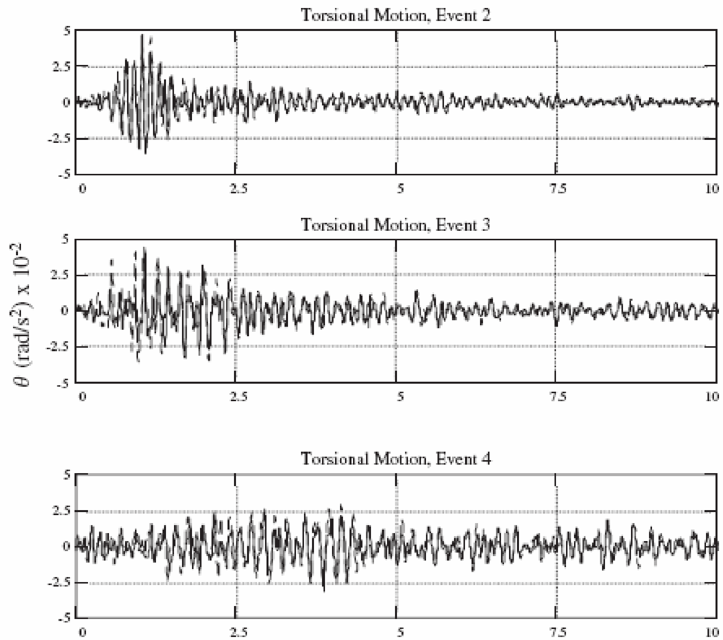

Ghayamghamian M.R. and Motosaka M., 2003, **The effects of torsion and motion coupling in site response estimation**, *Journal of Earthquake Engineering and Structural Dynamics,* Vol. 32, No. 5, pp. 691-709.

Translation and torsion motion couplings

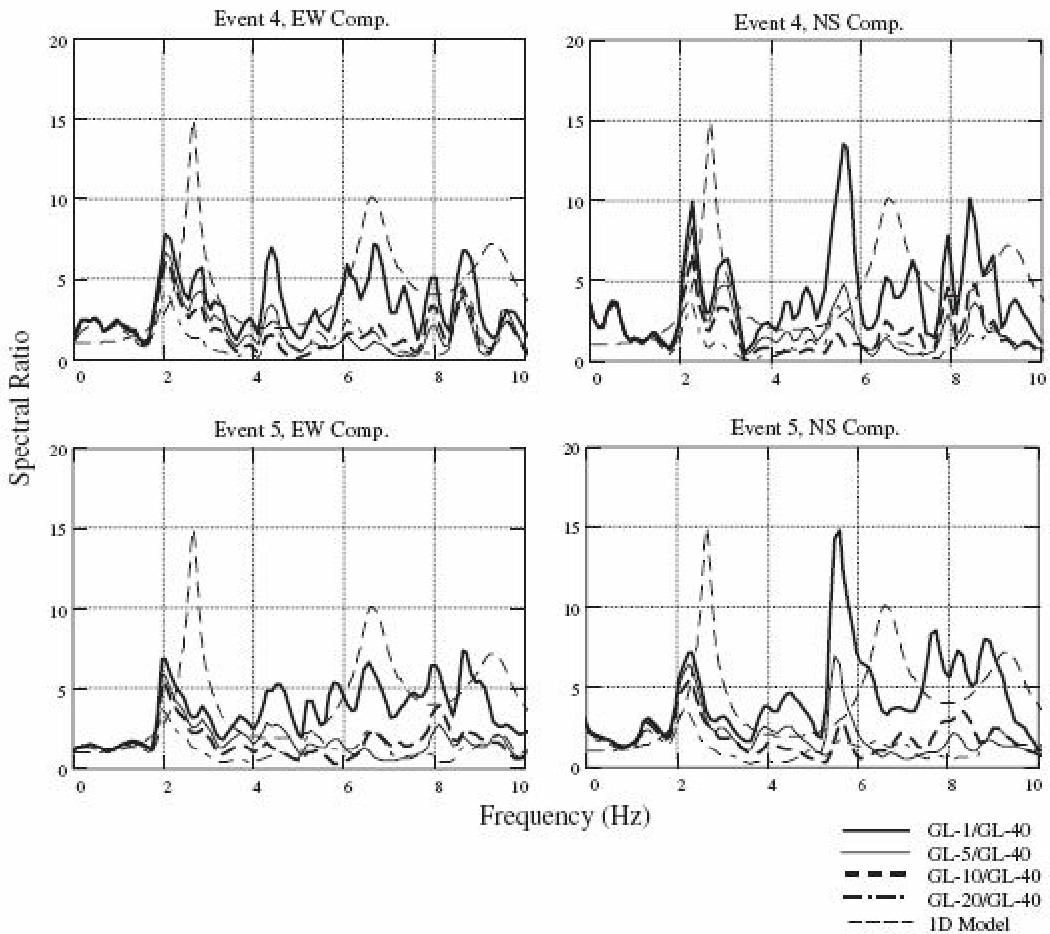

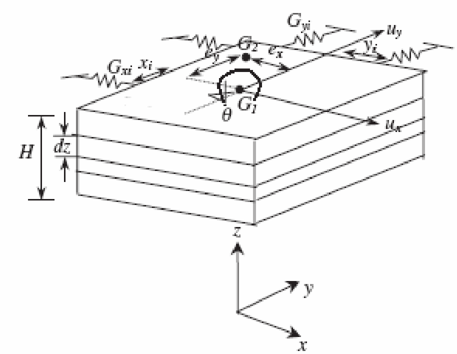

Schematic figure to explain the considered model for torsion and its parameters.

$$\begin{bmatrix} G_{xx} & G_{xy} & G_{x\theta} \\ G_{yx} & G_{yy} & G_{y\theta} \\ G_{\theta x} & G_{\theta y} & G_{\theta\theta} \end{bmatrix} \frac{\partial^2}{\partial z^2} \begin{Bmatrix} u_x \\ u_y \\ u_\theta \end{Bmatrix} = \begin{bmatrix} \rho & 0 & 0 \\ 0 & \rho & 0 \\ 0 & 0 & \rho \end{bmatrix} \frac{\partial^2}{\partial t^2} \begin{Bmatrix} u_x \\ u_y \\ u_\theta \end{Bmatrix}$$

$$\rho v_x^2 \begin{bmatrix} 1 & -\alpha & e_y \\ -\alpha & \gamma^2 & e_x \\ e_y & e_x & \beta^2 \end{bmatrix} \frac{\partial^2}{\partial z^2} \begin{Bmatrix} u_x \\ u_y \\ u_\theta \end{Bmatrix} = \begin{bmatrix} \rho & 0 & 0 \\ 0 & \rho & 0 \\ 0 & 0 & \rho \end{bmatrix} \frac{\partial^2}{\partial t^2} \begin{Bmatrix} u_x \\ u_y \\ u_\theta \end{Bmatrix}$$

$$\begin{bmatrix} 1 & -\alpha & e_y \\ -\alpha & \gamma^2 & e_x \\ e_y & e_x & \beta^2 \end{bmatrix} \frac{d^2}{dz^2} \begin{Bmatrix} \bar{u}_x \\ \bar{u}_y \\ \bar{u}_\theta \end{Bmatrix} = \begin{bmatrix} -\rho\omega^2 & 0 & 0 \\ 0 & -\rho\omega^2 & 0 \\ 0 & 0 & -\rho\omega^2 \end{bmatrix} \begin{Bmatrix} \bar{u}_x \\ \bar{u}_y \\ \bar{u}_\theta \end{Bmatrix}$$

Ghayamghamian and Motosaka (2003)
Ghayamghamian and Nouri (2007)

Sendai City and Seismic Network

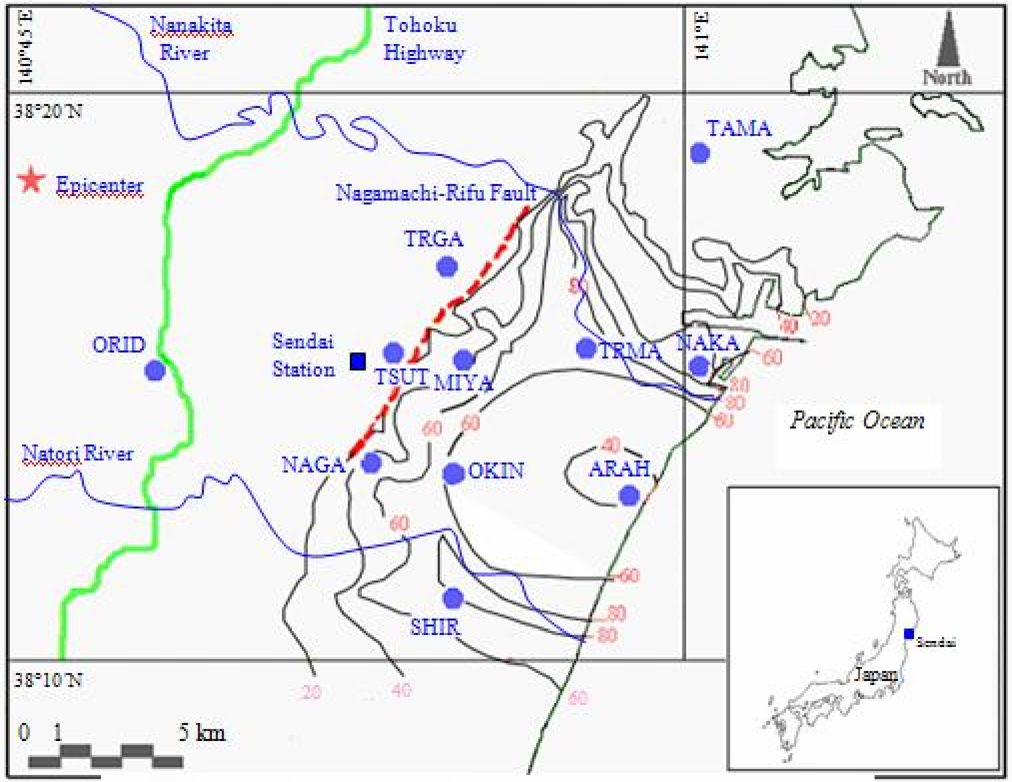

(a)

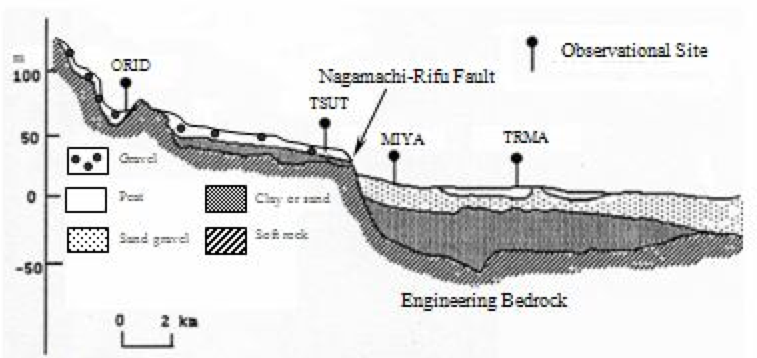

NS Comp. of Acc. Ground Motion Recorded at Different Locations Around Sendai Basin

List of Events with Parameters Determined by the Japan Meteorological Agency

Event Number	Origin Time (dd/mm/yyyy hh:mm)	Location	Depth (km)	M_{JMA}
19	09/15/1998 16:18	38.27° N, 140.76° E	9.2	3.8
20	09/15/1998 16:24	38.28° N, 140.76° E	13.3	5.0
21	09/15/1998 16:31	38.27° N, 140.75° E	10.1	3.6

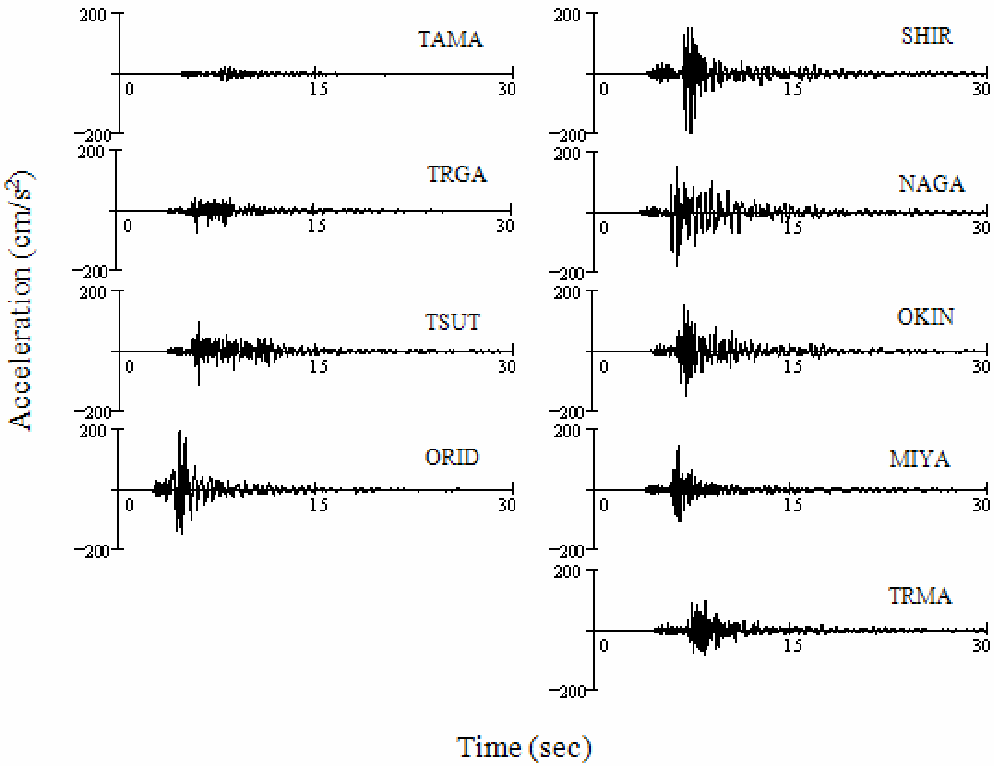

Soil Profile Based on Density and *S*-Wave Loggings at the Downhole Array Sites in Sendai

Number	Location of Accelerograms	Depth (m)	Soil Type	V_s (m/sec)	Density (kg/m³)
		MIYA Site			
1	▾ (−1)	1.0–1.5	Clay with rubble	210	1.60
2		1.5–3.0	Gravel with clay	350	1.90
3		3.0–11.0	Gravel with clay	430	1.90
4		11.0–22.0	Gravel with clay	480	2.00
5	▾ (−22)	22.0–25.5	Gravel with clay	540	2.00
6		25.5–34.0	Tuff, mudstone	540	1.80
7		34.0–39.9	Mudstone	570	1.80
8		39.9–46.0	Sandstone	570	1.90
9		46.0–52.7	Sandstone	480	1.90
10		52.7–54.0	Mudstone	480	1.80
11	▾ (−54)	54.0-	Shale	680	1.80
		NAGA Site			
1	▾ (−1)	1.0–4.9	Sand	105	1.65
2		4.9–9.3	Gravel	290	1.95
3		9.3–20.3	Sandy clay	170	1.70
4		20.3–28.5	Gravel with clay	290	1.75
5	▾ (−29)	28.5–56.5	Gravel with clay	600	2.10
6		81.0–56.5	Sandstone	530	1.95
7	▾ (−81)	81.0-	Sandstone	700	1.95
		OKIN Site			
1	▾ (−1)	1.0–6.0	Gravel ,Silt	130	1.60
2		6.0–8.0	Gravel	250	1.95
3		8.0–11.8	Gravel	470	2.00
4		11.8–13.9	Clay	220	1.65
5		13.9–16.7	Fine sand	220	1.80
6	▾ (−17)	16.7–22.0	Gravel	420	2.00
7		22.0–41.8	Gravel with clay	530	2.10
8		41.8–49.6	Gravel with clay	660	2.10
9		49.6–62.0	Sandstone	560	2.00
10	▾ (−62)	62.0-	Sandstone	820	2.00

Amplification Function Calculated by Uphole to Downhole Spectral Ratio, which reveal Coupling of shear wave around Basin Edge

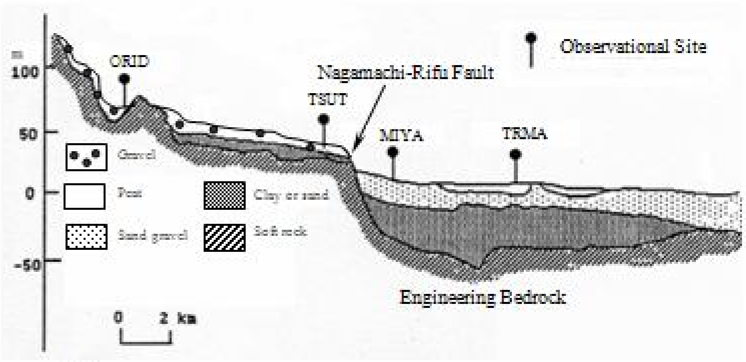

(b)

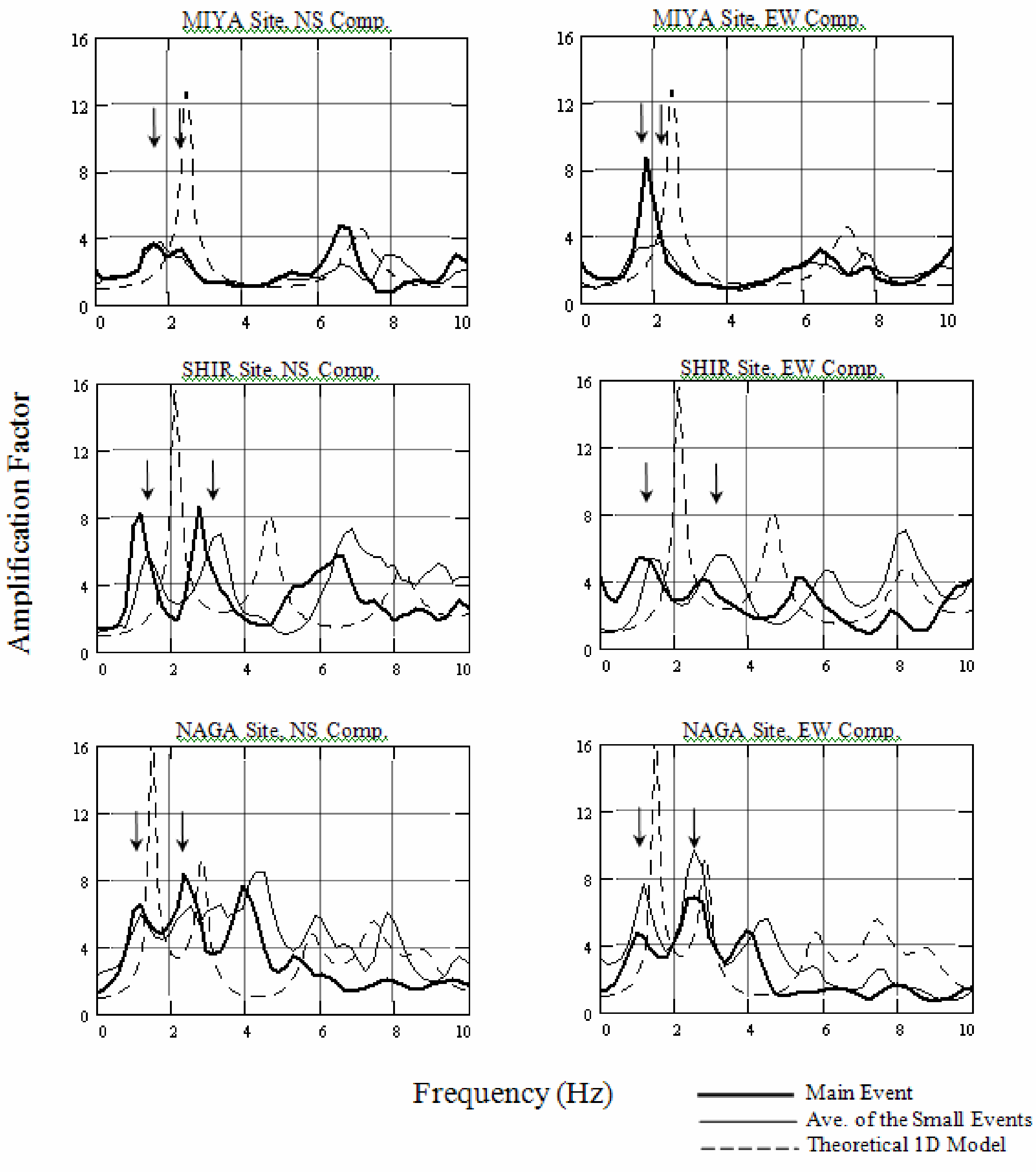

Ghayamghamian M.R., 2008, **Evidence for shear wave coupling due to small-scale lateral irregularities and its influence on site response estimation**, *Bulletin Seismological Society of America (BSSA)*, Vol. 98, No.3, pp. 1429-1446.

Estimating of Torsional motion using Sendai array data

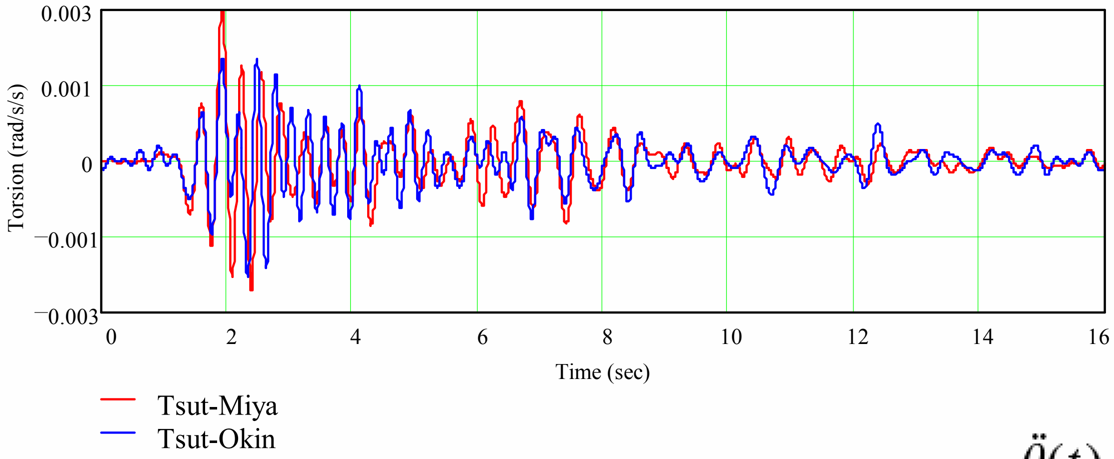

$$\ddot{\theta}(t) = \frac{1}{2}\left(\frac{\partial \ddot{u}(x,y,t)}{\partial y} - \frac{\partial \ddot{v}(x,y,t)}{\partial x}\right)$$

$$\ddot{\theta}(t) = \frac{1}{2}\left[\frac{\ddot{u}_2(t) - \ddot{u}_1(t)}{\Delta y} - \frac{\ddot{v}_2(t) - \ddot{v}_1(t)}{\Delta x}\right]$$

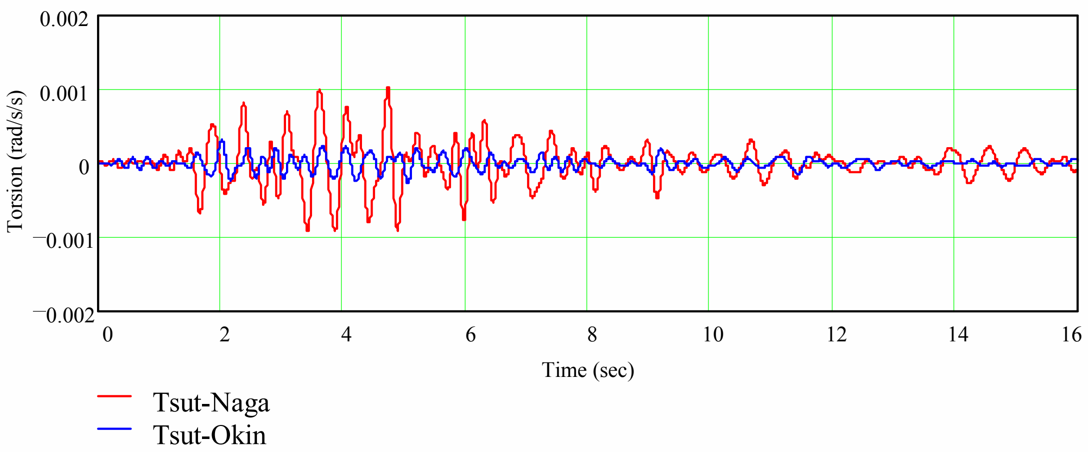

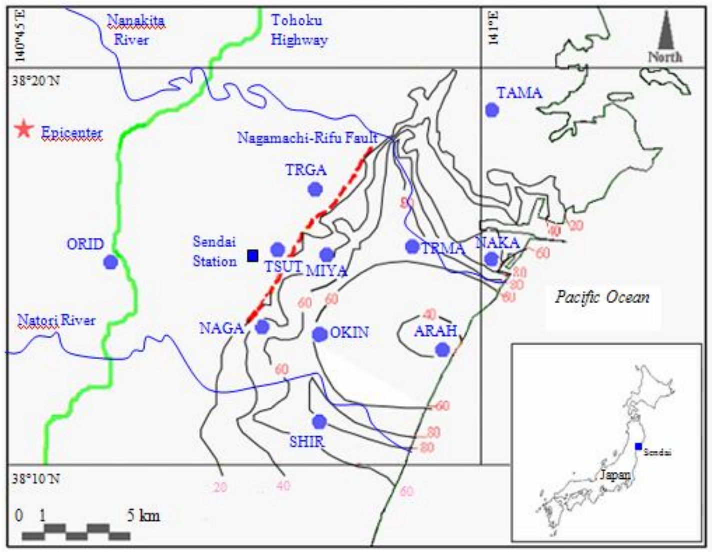

(a)

Torsional motion variations around Sendai Basin

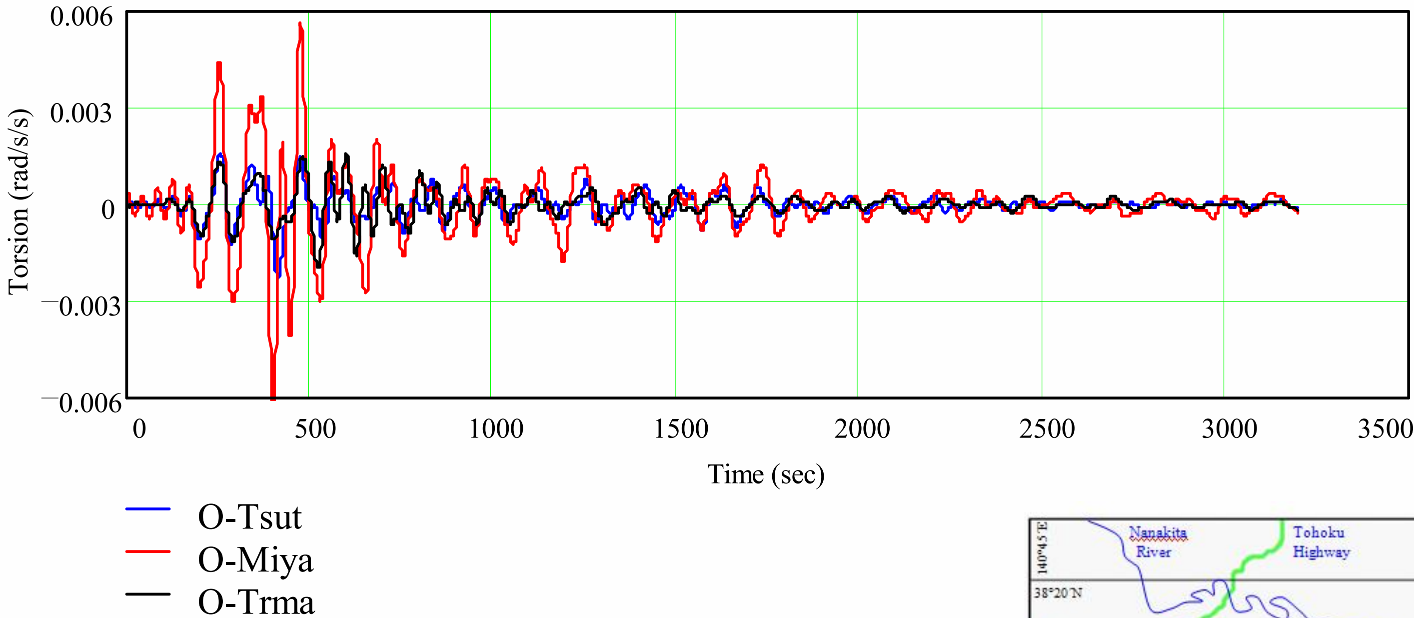

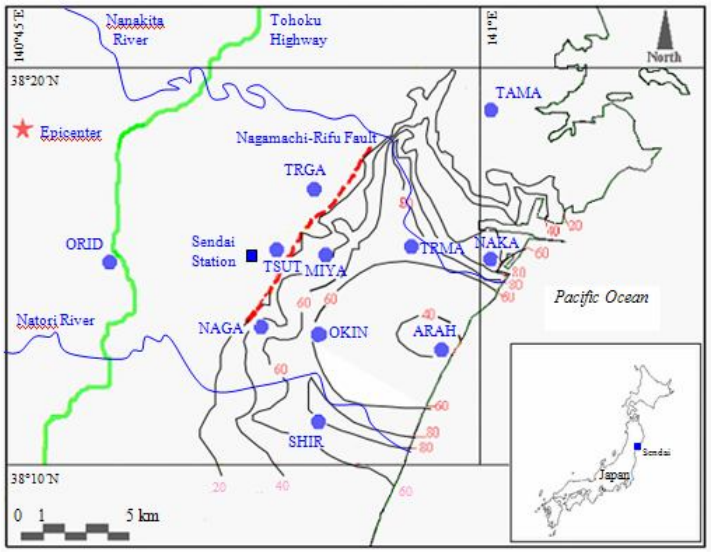

(a)

Numerical model for small-scale basin

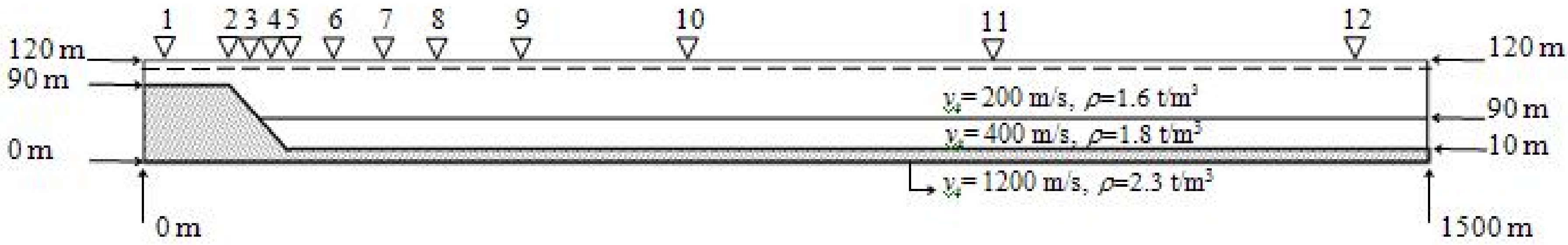

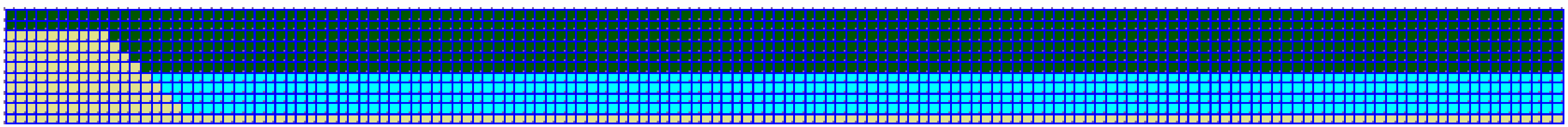

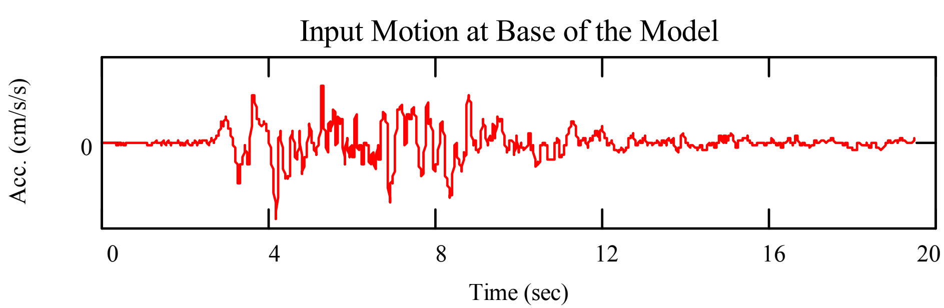

Calculated Acc. motion at surface for the points using FLIP program

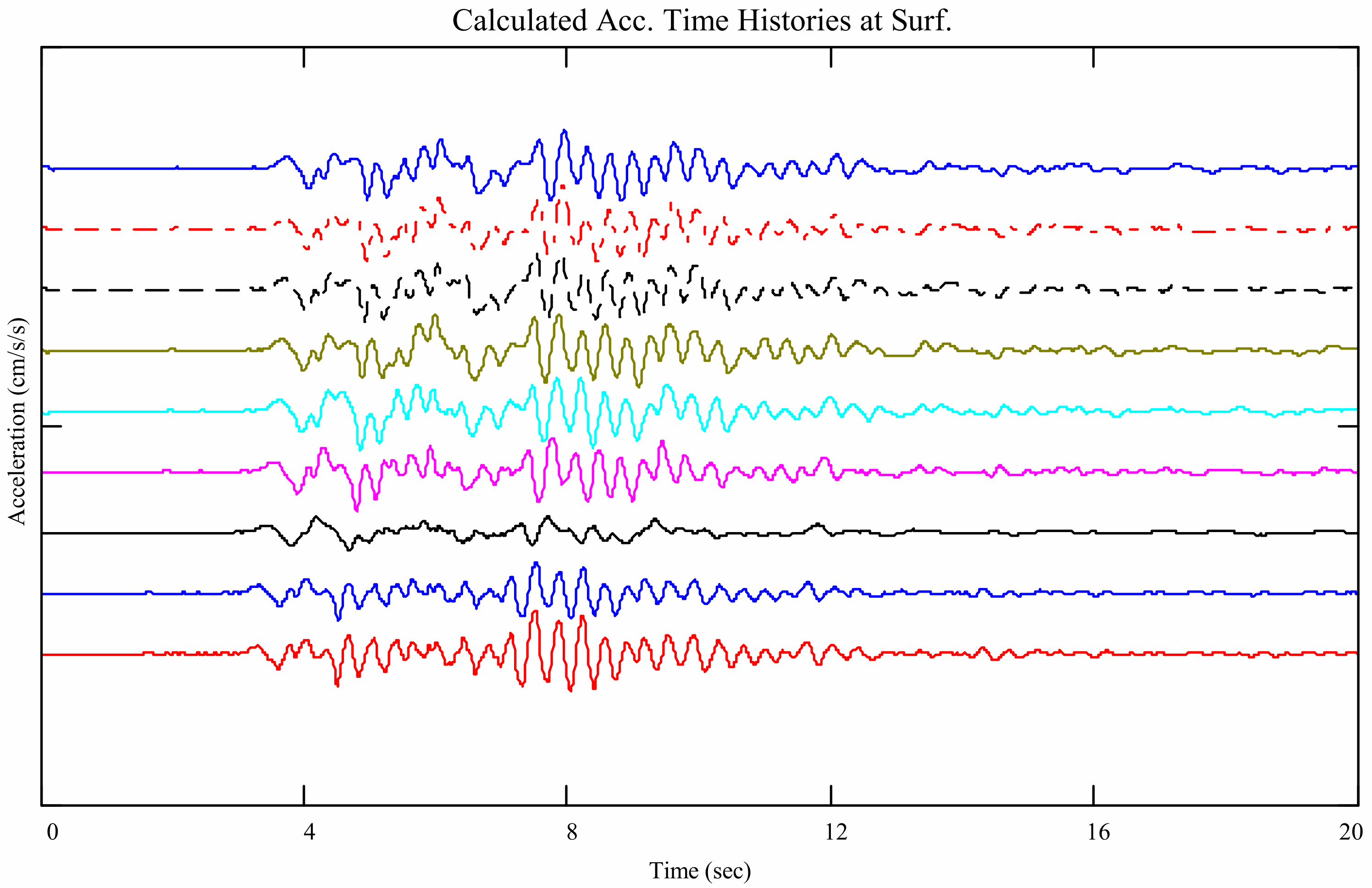

Torsional motion inferred from surface motions numerically calculated along the small-scale basin model.

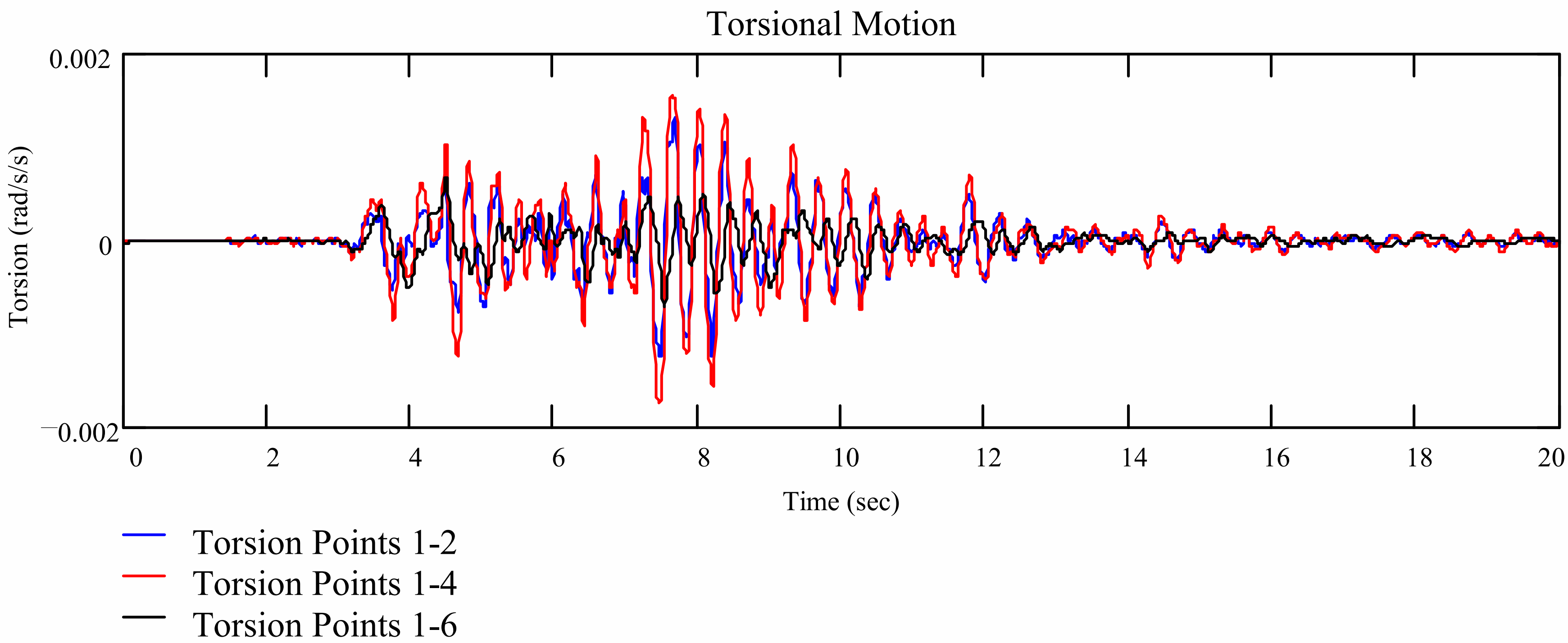

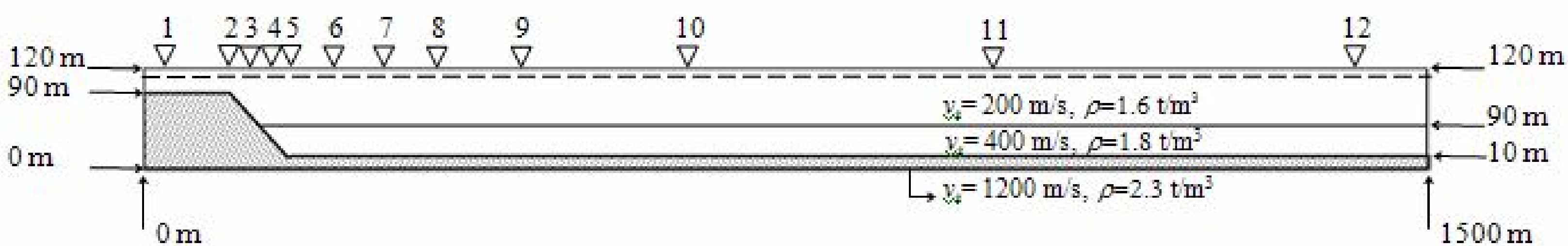

Some future works on the effect of Torsional motion using centrifuge test of the small-scale basin

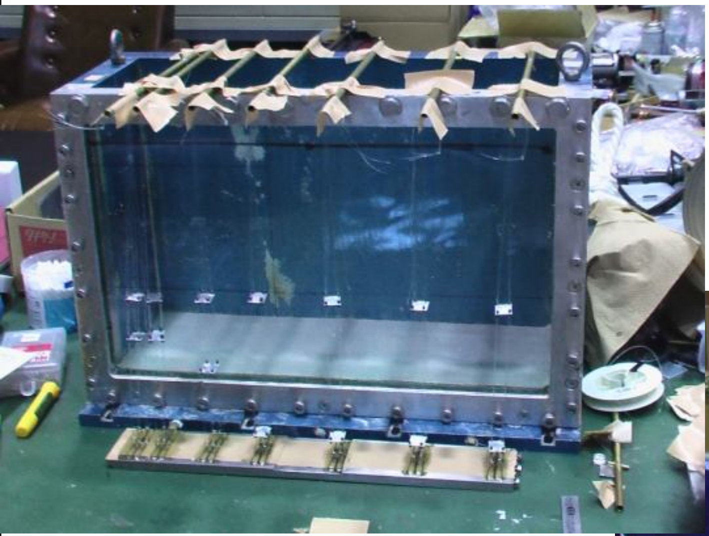

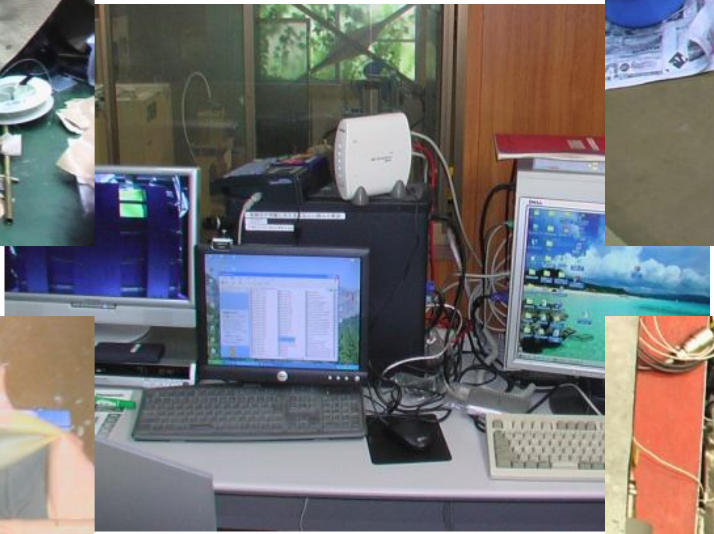

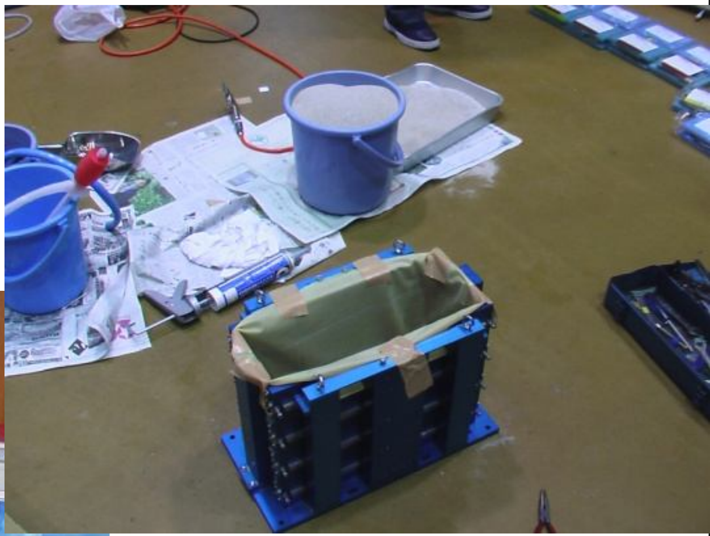

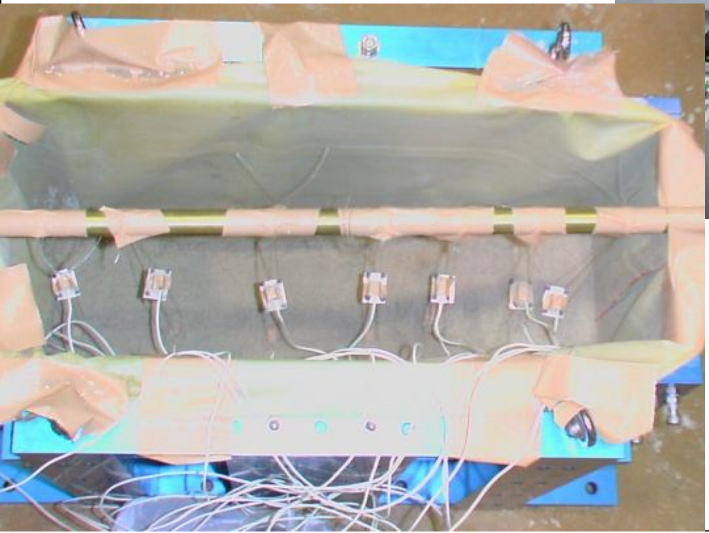

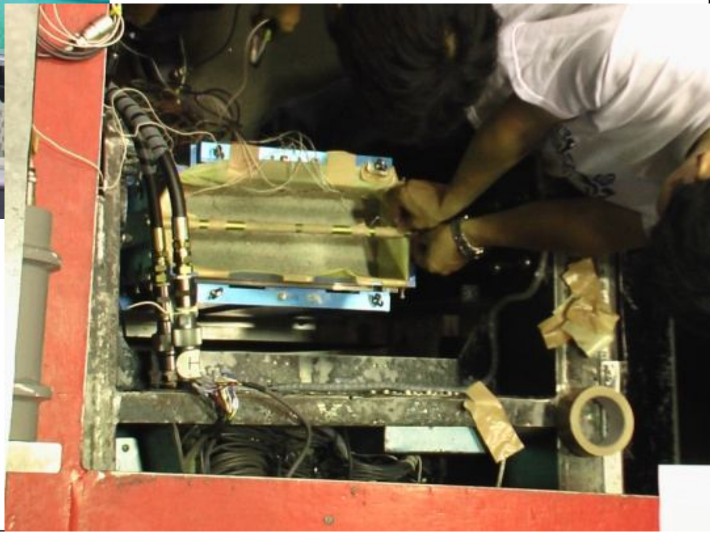

Conclusions

- The torsional motion affected by material and geometrical heterogeneity

- The small-scale basin (geometrical heterogeneity) caused large torsional motion around basin edge.

- This was verified through the anlysis of actual data from Sendai seismic array, and by numerical modeling.

Thank You For Your Attention